

Glycol-Thermal Continuous Flow Synthesis of Graphene Gel

Luke C.O. Prestowitz and Jiaxing Huang*

Cite This: *ACS Omega* 2021, 6, 18663–18667

Read Online

ACCESS |



Metrics & More

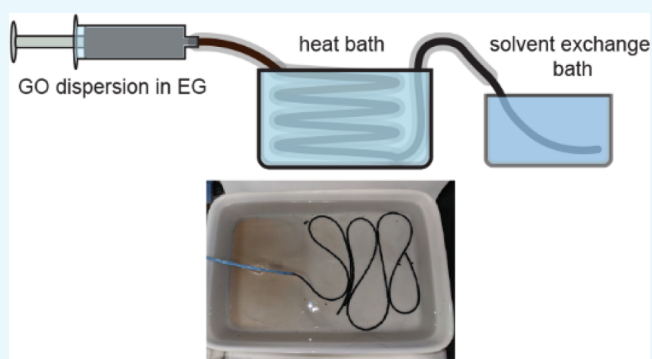


Article Recommendations



Supporting Information

ABSTRACT: Hydrothermal treatment of graphene oxide (GO) aqueous dispersion has been extensively applied to create graphene (a.k.a., chemically modified graphene, or reduced GO) hydrogels, which were dried to yield high-density graphene monoliths and powders with promising potential for electrochemical energy storage applications. Here, we demonstrated a glycol-thermal route that allows the preparation of a graphene gel at around 150 °C, which is below the boiling point of ethylene glycol (EG) and thus eliminates the need for a sealed pressurized reaction vessel. As a result, flow synthesis can be achieved by flowing a GO dispersion in EG through a Teflon tube immersed in a preheated oil bath for continuous production of a graphene gel, which, upon drying, shrinks to yield a densified graphene solid.



INTRODUCTION

Graphene oxide (GO) is the product of chemical exfoliation of graphite powders,¹ and can be obtained as a colloidal dispersion in water with high single-layer yield and large lateral sizes. The insulating GO can be conveniently converted to its conductive form of reduced GO (r-GO, a.k.a., chemically modified graphene) through many thermal, chemical, and light-based methods.² Therefore, GO has been used as a water-processible precursor to create bulk forms³ of graphene-based materials including fibers,^{4,5} films,^{6–8} foams,^{9,10} gels,^{10–13} and densified solids.^{11–16} Among them, densified graphene monoliths or powders, with largely isotropically packed sheets, have been shown to have interesting chemical,¹⁶ mechanical,¹⁵ and electrochemical properties.¹⁴ Such isotropic graphene solids are typically made by slow drying of the corresponding graphene hydrogels obtained by hydrothermal treatments of GO dispersions.¹⁰ The gel network, formed by the sheets in the hydrogel, is crumpled and densely packed under capillary compression^{3,14,17} to yield the final high-density solids.^{11–13}

In the hydrothermal gelation process, a GO dispersion of relatively high concentration is heated well over the boiling point of water to trigger the deoxygenation reaction of GO. Because the resulting reduced GO sheets are less dispersible in water, they gradually aggregate and assemble into a network, forming a hydrogel during undisturbed cooling.^{10,18} Because the temperatures typically used to induce the hydrothermal sol–gel transition^{10,18} occurs well above the boiling point of water, a sealed pressurized vessel is needed to contain the reaction, constraining the synthesis to batch processing and making it harder to scale up. Larger reaction vessels do yield larger hydrogels, which, however, are prone to collapse due to

their own weight, and nonuniform drying can lead to cracking and inhomogeneous microstructures.

It is worth noting that in hydrothermal sol–gel transition of GO, the need for a pressurized vessel is not a necessity for gelation, but an inconvenient consequence of needing to contain the aqueous dispersion above its boiling point. Therefore, if GO can be heated over its deoxygenation reaction temperature in a high boiling point solvent, reduction^{19,20} and gelation should occur at ambient pressure. Here, we demonstrate that a graphene gel can indeed form by heating an ethylene glycol (EG) dispersion of GO. This glycol-thermal sol–gel transition is accompanied by a slight volume shrinkage, making the graphene glycol-gel suspend in the solvent. This inspired and enabled a hyperloop-like²¹ flow synthesis, as the glycol-gel can flow freely and continuously through a tube without being abraded by the tube wall.

RESULTS AND DISCUSSION

As illustrated by the drawings in Figure 1a,b, hydrothermal gelation of GO involves a high-pressure autoclave, in which the GO solution forms a gel, which shrinks with the reaction time. The gel can be directly dried to form a compact and densified graphenic solid (Figure 1c,d). To make clear that high pressure is not essential to the formation of a gel, a GO/water solution (1 mg mL⁻¹) was heated at 98 °C with a plastic cap covering

Received: May 17, 2021

Accepted: July 5, 2021

Published: July 14, 2021



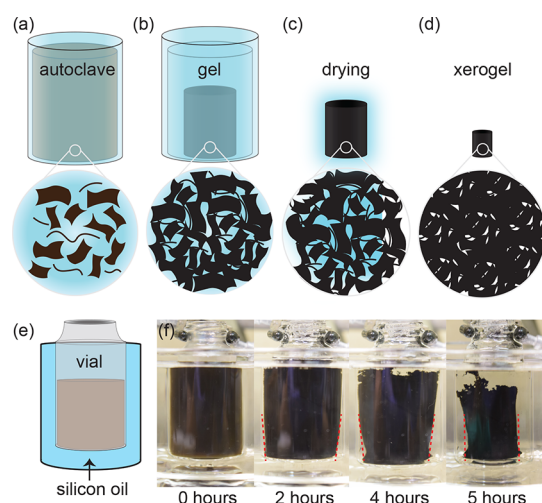


Figure 1. Comparison of the graphene gel synthesis by the conventional pressurized hydrothermal reduction and the alcohol thermal reduction at ambient pressure. (a) In the hydrothermal reactor, aqueous GO dispersion turns into (b) a graphene hydrogel after heating in a sealed vessel at above 150 °C. (c) Hydrogel shrinks upon drying in air and eventually densifies into (d) a xerogel made of densely packed but highly disordered sheets. (e,f) GO dispersion in EG is gelled in a 150 °C silicone oil bath, and eventually forms an graphene algogel during the reduction and syneresis (red-dotted lines). No pressure vessel is needed.

the container, loosely, to avoid complete evaporation of water. A soft gel indeed formed successfully after 24 h, which confirmed that high pressure is not needed for gel formation. On the other hand, the obtained gel was very brittle and weak, making subsequent handling and processing difficult, suggesting that a high temperature, rather than high pressure, is necessary for obtaining a stiff gel within a short-time frame. Therefore, the optimal solvent for the formation of a graphene gel at ambient pressure should be capable of dispersing GO while also having a high boiling point. One of the solvents meeting these requirements is EG.²²

First, we tested whether a graphene gel can be produced in EG. A 20 mL scintillation vial filled with 0.1 wt % GO/EG solution was placed into a preheated silicon oil bath (150 °C) (Figure 1e), which allows direct visual observation throughout the solvothermal process (Figure 1f). Gelation indeed occurred and was accompanied by syneresis, leading to the suspension of a slightly shrunken gel in the expelled solvent. In the experiment, the vial was intentionally uncapped, clearly showing that high pressure is not necessary for gel formation.

Observations made in Figure 1e,f inspired the design of a flow synthesis of a graphene gel. Because the sol–gel transition is accompanied by a drastic increase in viscosity, flow synthesis of gel in a tube reactor would be difficult because the drag on the gel by the inner wall not only increases the resistance but also continuously deforms and damages the gel. Because the graphene glycol-gel undergoes syneresis, the gel should stay “levitated” and flow drag-free inside the tube, just like a hyperloop train inside a tunnel.²¹ This should lead to the continuous and smooth extrusion of a graphene gel without getting stuck by friction with the tube (Figure 2b). A polytetrafluoroethylene (PTFE) tube was used as the flow reactor due to its thermal and chemical stability, as well as low surface energy. The graphene gels with different diameters ranging from around 3.2–12.7 mm can be obtained depending

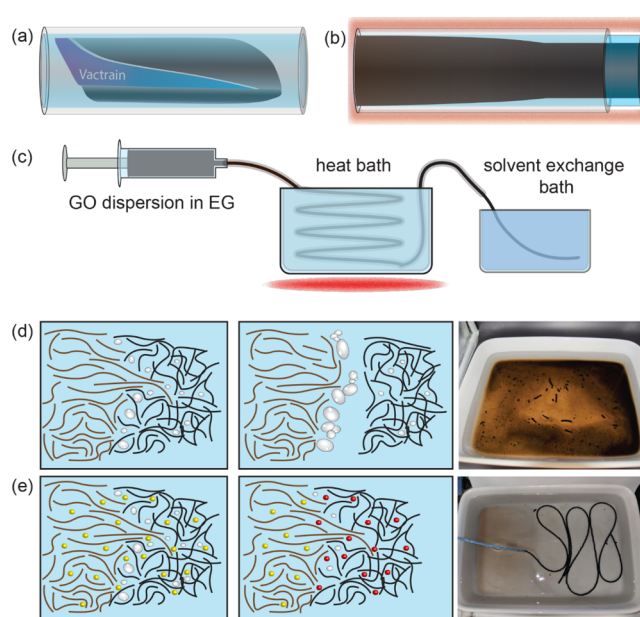


Figure 2. Continuous flow synthesis of graphene gel by the alcohol thermal reduction method. (a) Schematic drawing illustrating the concept of a vactrain (e.g., hyperloop), which travels through a tube without any direct contact with the wall due to magnetic levitation. (b) Similarly, syneresis during the sol–gel transition allows the gel to be “levitated” in the solvent and glide through a tube without any drag or friction with the tube wall, as illustrated in (c) the continuous flow, “glycol-thermal” reaction setup. (d) CO₂ bubbles (white) released during the formation of reduced GO can rapidly expand when they are heated inside the tube, causing uncontrolled bursts, which push the solution out of the tube prematurely, before it has a chance to form a continuous gel. (e) Adding NaOH (yellow dots) to the reaction helps to sequester the CO₂ gas by forming Na₂CO₃ (red dots), allowing uninterrupted gelation of graphene that can be extruded continuously.

on the inner diameter of the tubes. For the sake of simplicity, all the discussion from this point forward refers to gels with a diameter of 3.2 mm.

As a proof-of-concept, a 6 mg mL⁻¹ GO/EG solution was injected into a PTFE tubing at a rate of 45 mL h⁻¹ controlled by a syringe pump (Figure 2c). The coiled tubing is completely submerged into a silicon oil heating bath maintained at 150 °C, resulting in a residence time of the GO of approximately 22 min. Thermal deoxygenation of GO and gelation of the sheets occurs quickly, with the color changing from brown to black. However, along with the formation of the gel, the generated gas grows into large bubbles at the sol–gel transition interface. These bubbles eventually coalesce to bisect the tube, breaking the glycol-gel from the GO solution. Once the gel is separated, the pressure from the trapped gas pocket rapidly ejects the as-formed glycol-gel out of the tube (Figure 2d). Evidently, the gaseous byproducts have insufficient solubility in the solvent.²³ To address this problem, the continuous extrusion of gels can be achieved by sequestering carbon dioxide, which is the major component of the released gas, using sodium hydroxide to neutralize and convert any generated carbon dioxide to sodium carbonate (Figure 2e). The salt, together with the EG, can be removed by a solvent exchange process with deionized (DI) water. The solvent exchange is repeated four times over a 48 hour period.

The obtained graphene gels can be dried by freeze-drying to maintain the microstructure, or natural drying to yield the

densified xerogel after solvent exchange with water. The freeze-dried aerogel shows a low-density foam structure as seen in the cross-sectional scanning electron microscopy (SEM) image (Figure 3a). The freeze-dried aerogel can be densified by

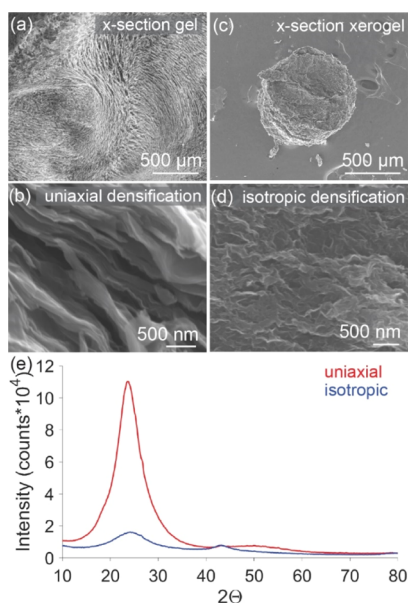


Figure 3. Gel and xerogel characterization. (a) Cross-sectional SEM image of the as-extruded graphene glycol gel showing its low-density foam-like structure. (b) After uniaxial compression, the foam turns into a dense anisotropic lamellar structure. (c) When the purified gel from (a) is dried under ambient conditions, it undergoes isotropic compression because of the solvent drying and (d) xerogel structure is significantly crumpled and twisted. (e) As a result of these densification methods, two different microstructures are generated, as seen in the X-ray diffraction patterns, where the greater degree of restacking of graphene sheets occurs in the uniaxially pressed condition versus the isotropic drying.

uniaxial compression, which yields a dense solid with an anisotropic lamellar microstructure (Figure 3b). Slow drying of the graphene gel in air subjects the sheets to a largely isotropic compressive force field, and the resulting microstructure of the xerogel is made of densely yet disorderly packed crumpled sheets (Figure 3c,d). The lack of long-range stacking order in the graphene xerogel is confirmed by the significantly weaker (002) peak compared to the uniaxially densified graphene solid in the X-ray diffraction patterns (Figure 3e). The XRD pattern of the naturally dried xerogel powder is similar to that of the graphenic glass presented in previous work,¹⁵ indicating that these xerogel powders may be used as a building block for making larger bulk graphenic materials.

As was stated above, a substantial amount of the byproducts can be removed by a 2 day solvent exchange, however, some sodium carbonate may still be present (Figure S1a). Purification can be accelerated by soaking the xerogel in concentrated sulfuric acid overnight. Concentrated sulfuric acid, which is used in the synthesis of GO, intercalates the tightly packed graphene sheets and swells the xerogel, removing the excess sodium carbonate at the same time (Figure S1b).²⁴ Even though prolonging the solvent exchange with DI water can also achieve a high purity of the xerogel, for this report, the sulfuric acid method was utilized. After a thorough dilution and rinse, the purified xerogel can be

obtained after drying at room temperature with a density of $1.63 \pm 0.08 \text{ g cm}^{-3}$.

The chemical composition including carbon, hydrogen, oxygen, and nitrogen of the as-extruded and purified xerogel powder was evaluated by combustion-based elemental analysis. The sulfur content was found to be negligible, indicating thorough removal of sulfuric acid by the final rinsing step. Given that the atom ratio of carbon to oxygen is approximately 2.8, the starting GO is not highly reduced during extrusion. Despite its low reduction state, which may be attributed to the short time spent in the heated silicon oil bath, it still performs well as an electrode material for supercapacitors (Figure S2). If it is further annealed (e.g., at $350 \text{ }^\circ\text{C}$ for 1 h), the conductivity of the xerogel powder can be improved (Table S1), which contributes to an enhancement in performance. As demonstrated in Figure 4a, the annealed xerogel powder exhibits a

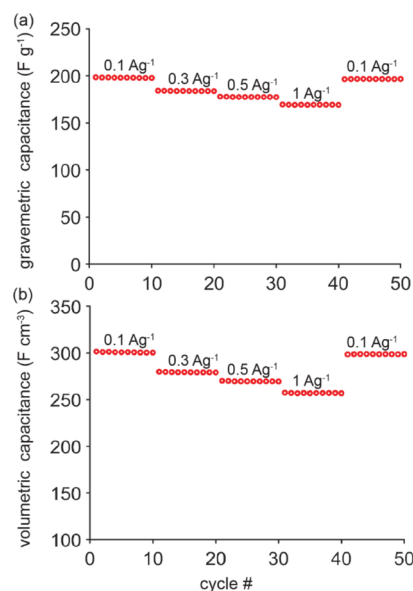


Figure 4. Electrochemical performance of the optimized graphene xerogel in a coin cell supercapacitor. (a) Gravimetric performance. (b) Volumetric performance.

gravimetric capacitance of 198 F g^{-1} at a current density of 0.1 A g^{-1} , and maintains a respectable value at higher current densities. Based on the xerogel powder's density of $1.52 \pm 0.07 \text{ g cm}^{-3}$, the volumetric capacitance is estimated to be around 300 F cm^{-3} . The gravimetric and volumetric capacitances are comparable to those reported in previous reports based on hydrothermal graphene hydrogels, which showed that densified graphene powders are promising materials for developing supercapacitors with a high energy density.^{13,14} In addition, the quasirectangular cyclic voltammetry curves and electrochemical impedance spectroscopy show good capacitive behavior and low resistance of the graphene xerogel powders (Figures S3 and S4). Consequently, the continuous flow synthesis holds promise to make scalable graphene powders for applications in energy storage devices.

CONCLUSIONS AND OUTLOOK

The shrinkage of the graphene gel during glycol-thermal treatment simultaneously expels excess solvent and suspends the gel. This enables a flow synthesis of graphene glycol-gels using high boiling point solvents such as EG without the need

to seal and pressurize the reaction vessel. Syneresis during the sol–gel transition of GO in a heated tube reactor allows continuous extrusion of the graphene glycol-gel product. Sodium hydroxide can be added to the dispersion to neutralize and capture released CO₂ in the reaction. After solvent exchange to replace EG and remove the salt byproducts, the purified graphene gel can then dry in air to yield a densified xerogel, which is made of densely and yet disorderly packed crumpled sheets. This flow synthesis method could be extended to prepare a number of GO-based multifunctional composite materials, leveraging GO's surfactant-like properties^{25–27} to codisperse other materials such as carbon nanomaterials,²⁸ conductive polymers,^{29,30} biomass,³¹ silicon,³² metal³³ and oxide³⁴ nanoparticles, and many others. As a proof-of-concept, a coextrusion with polyaniline nanofibers, nickel, and carbon black (CB) was achieved (Figure S5). The xerogel powders may be useful for electrochemical energy storage applications or may be used as a building block for making larger bulk graphenic glass materials.

■ EXPERIMENTAL METHODS

Low-Temperature Hydrogel Formation. 80 mL of a 0.1 wt % GO solution was placed in a 100 mL beaker. The beaker was then placed in an oven at 98 °C and a plastic cover was placed on top. It was left for 24 h, after which a hydrogel had formed.

Synthesis of Glycol-Gel in a Vial. A GO dispersion of 2 mg mL⁻¹ in EG was prepared, which contained 4–5% of water. 18 mL of this dispersion was added into a glass scintillation vial, which was suspended in a silicon oil bath heated to 150 °C. No stirring was applied. Time-lapse photographs were taken during the gelation process.

Continuous Flow Synthesis. Optimized syntheses used a 6 mg mL⁻¹ of GO dispersion in EG containing 4% of water, to which 0.1 M NaOH was added immediately before extrusion. This solution was then collected in a 60 mL syringe, which was attached to a PTFE tube of 3.2 mm in diameter. The tube was coiled three times for a total length of approximately 1.25 m and placed in a silicon oil bath set to 150 °C. The solution was pumped through the tube using a syringe pump set to a rate of 45 mL h⁻¹, which corresponds to a linear flow rate of ~568 cm h⁻¹ and an overall traveling time of about 22 min through the entire heated length of the tube. The extruded gel was collected in a 2 L glass beaker filled with DI water. To purge the remaining r-GO gel in the tube after the syringe had been emptied, a new syringe filled with pure EG was placed into the pump.

Solvent Exchange. The 2 L beaker in which the glycol-gel had been extruded was kept in an oven at 60 °C for 4 h before replenishing water. This cycle was usually repeated four times over a 2 day period. After the final rinse, the gel was dried at room temperature to generate a xerogel. This xerogel can then be ground into powders.

Sulfuric Acid Soak. To accelerate the removal of excess sodium carbonate salt, the xerogel powders are soaked in concentrated sulfuric acid in an oven at 60 °C overnight, followed by rinsing with DI water before filtration and drying.

Supercapacitor Assembly and Testing. The purified xerogel powder is then mixed with a 10:1:1 ratio by mass of xerogel powder, Super P, and PTFE binder, respectively. They are all mixed in a mortar and pestle and transferred to a PTFE slab, where it is rolled out into a single film. Once the film is dried, it is transferred to a nickel foam electrode and pressed at

1 MPa. The electrode is then placed with a symmetric pair in a coin cell and a fine pore filter paper is used as a separation membrane. To this, 6 M KOH electrolyte is added, and the coin cell is pressed at 1 MPa.

The coin cell is then placed in a NEWARE battery cell tester, where it is run at 0.1, 0.3, 0.5, 1, and back to 0.1 A/g for 10 cycles each. The capacitance is calculated using the following formula

$$C_s = \frac{2I\Delta t}{m\Delta V}$$

where C_s is the specific capacitance of the electrode, I is the discharge current, Δt is the discharge time in seconds, m (g) is the mass of the electrode, and ΔV is the potential window of the discharge process after the IR drop.

Elemental Analysis. Samples were shipped to Atlantic Microlab in Norcross, GA for CHS composition analysis.

X-ray Diffraction. The xerogel powders and the uniaxially compressed r-GO foam were placed on a zero-diffraction plate, and the diffraction pattern was collected on a Rigaku SmartLab X-ray diffractometer using a monochromatic Cu $K\alpha$ 1, 2 (no Cu $k\beta$) source at 45 kV and 160 mA.

Polyaniline Nanofiber Coextrusion. Doped polyaniline nanofibers³⁵ were mixed into the EG/GO solution at 0.5 mg mL⁻¹ using bath sonication for 15 min. This solution was then used in the continuous flow synthesis procedure.

CB Coextrusion. Alfa Aesar CB (Super P conductive; 99+ % (metals basis) [1333-86-4]) was added at a mass ratio of 10:1 GO/CB into the EG/GO solution prior to extrusion. It was then mixed using bath sonication for 15 min. This solution was then used in the continuous flow synthesis procedure.

Nickel Powder Coextrusion. 1 mg mL⁻¹ nickel powder (3 μ m; 99.7% trace metal basis powder) from Sigma-Aldrich [7440-02-0] was added into the EG/GO solution prior to extrusion. It was then mixed using bath sonication for 15 min. This mixture was then used in the continuous flow synthesis procedure.

■ ASSOCIATED CONTENT

Supporting Information

The Supporting Information is available free of charge at <https://pubs.acs.org/doi/10.1021/acsomega.1c02589>.

Results of microscopy observation of the xerogel before and after sulfuric acid treatment; electrochemical performance of the as-extruded graphene xerogel after solvent exchange in water; extended electrochemical characterization; proof-of-concepts of flow synthesis of graphene-based composites with polyaniline nanofibers, nickel metal powders, and CB particles; and conductivity of the xerogel samples before and after annealing (PDF)

■ AUTHOR INFORMATION

Corresponding Author

Jiaying Huang – Department of Materials Science and Engineering, Northwestern University, Evanston, Illinois 60208, United States; orcid.org/0000-0001-9176-8901; Email: jiaying-huang@northwestern.edu

Author

Luke C.O. Prestowitz – Department of Materials Science and Engineering, Northwestern University, Evanston, Illinois 60208, United States; orcid.org/0000-0002-3785-8954

Complete contact information is available at:
<https://pubs.acs.org/10.1021/acsomega.1c02589>

Notes

The authors declare the following competing financial interest(s): An invention disclosure related to this work has been submitted to Northwestern University, who may choose to file a patent application.

ACKNOWLEDGMENTS

This work was supported by the Office of Naval Research (ONR N000142012190). This work made use of the EPIC facility of Northwestern University's NUANCE Center and the Jerome B. Cohen X-Ray Diffraction Facility, which have received support from the SHyNE Resource (NSF ECCS-2025633), the IIN, and Northwestern's MRSEC program (NSF DMR-1720139). The author would like to thank Dr. Zhilong Yu for extensive discussions and assistance in improving the manuscript, and Dr. Hun Park, Dr. Pan He, and Haiyue Huang for their technical assistance and problem-solving conversations.

REFERENCES

- (1) Hummers, W. S.; Offeman, R. E. Preparation of Graphitic Oxide. *J. Am. Chem. Soc.* **1958**, *80*, 1339.
- (2) Pei, S.; Cheng, H.-M. The Reduction of Graphene Oxide. *Carbon* **2012**, *50*, 3210–3228.
- (3) Luo, J.; Gao, J.; Wang, A.; Huang, J. Bulk Nanostructured Materials Based on Two-Dimensional Building Blocks: A Roadmap. *ACS Nano* **2015**, *9*, 9432–9436.
- (4) Li, M.; Lian, J. Microstructure Dictating Performance: Assembly of Graphene-Based Macroscopic Structures. *Acc. Mater. Res.* **2021**, *2*, 7–20.
- (5) Park, H.; Lee, K. H.; Kim, Y. B.; Ambade, S. B.; Noh, S. H.; Eom, W.; Hwang, J. Y.; Lee, W. J.; Huang, J.; Han, T. H. Dynamic Assembly of Liquid Crystalline Graphene Oxide Gel Fibers for Ion Transport. *Sci. Adv.* **2018**, *4*, No. eaau2104.
- (6) Huang, Y.; Wang, C.; Shao, C.; Wang, B.; Chen, N.; Jin, H.; Cheng, H.; Qu, L. Graphene Oxide Assemblies for Sustainable Clean-Water Harvesting and Green-Electricity Generation. *Acc. Mater. Res.* **2021**, *2*, 97–107.
- (7) Cheng, L.; Liu, G.; Zhao, J.; Jin, W. Two-Dimensional-Material Membranes: Manipulating the Transport Pathway for Molecular Separation. *Acc. Mater. Res.* **2021**, *2*, 114–128.
- (8) Dikin, D. A.; Stankovich, S.; Zimney, E. J.; Piner, R. D.; Dommett, G. H. B.; Evmenenko, G.; Nguyen, S. T.; Ruoff, R. S. Preparation and Characterization of Graphene Oxide Paper. *Nature* **2007**, *448*, 457–460.
- (9) Jiang, Y.; Wang, Y.; Xu, Z.; Gao, C. Conformation Engineering of Two-Dimensional Macromolecules: A Case Study with Graphene Oxide. *Acc. Mater. Res.* **2020**, *1*, 175–187.
- (10) Xu, Y.; Sheng, K.; Li, C.; Shi, G. Self-Assembled Graphene Hydrogel Via a One-Step Hydrothermal Process. *ACS Nano* **2010**, *4*, 4324–4330.
- (11) Worsley, M. A.; Charnvanichborikarn, S.; Montalvo, E.; Shin, S. J.; Tylski, E. D.; Lewicki, J. P.; Nelson, A. J.; Satcher, J. H.; Biener, J.; Baumann, T. F.; Kucheyev, S. O. Toward Macroscale, Isotropic Carbons with Graphene-Sheet-Like Electrical and Mechanical Properties. *Adv. Funct. Mater.* **2014**, *24*, 4259–4264.
- (12) Bi, H.; Yin, K.; Xie, X.; Zhou, Y.; Wan, N.; Xu, F.; Banhart, F.; Sun, L.; Ruoff, R. S. Low Temperature Casting of Graphene with High Compressive Strength. *Adv. Mater.* **2012**, *24*, 5124–5129.
- (13) Tao, Y.; Xie, X.; Lv, W.; Tang, D.-M.; Kong, D.; Huang, Z.; Nishihara, H.; Ishii, T.; Li, B.; Golberg, D.; Kang, F.; Kyotani, T.; Yang, Q.-H. Towards Ultrahigh Volumetric Capacitance: Graphene Derived Highly Dense but Porous Carbons for Supercapacitors. *Sci. Rep.* **2013**, *3*, 2975.
- (14) Qi, C.; Luo, C.; Tao, Y.; Lv, W.; Zhang, C.; Deng, Y.; Li, H.; Han, J.; Ling, G.; Yang, Q.-H. Capillary Shrinkage of Graphene Oxide Hydrogels. *Sci. China Mater.* **2020**, *63*, 1870.
- (15) Yeh, C.-N.; Huang, H.; Lim, A. T. O.; Jhang, R.-H.; Chen, C.-H.; Huang, J. Binder-Free Graphene Oxide Doughs. *Nat. Commun.* **2019**, *10*, 422.
- (16) Klemeyer, L.; Park, H.; Huang, J. Geometry-Dependent Thermal Reduction of Graphene Oxide Solid. *ACS Mater. Lett.* **2021**, *3*, 511–515.
- (17) Luo, J.; Jang, H. D.; Sun, T.; Xiao, L.; He, Z.; Katsoulidis, A. P.; Kanatzidis, M. G.; Gibson, J. M.; Huang, J. Compression and Aggregation-Resistant Particles of Crumpled Soft Sheets. *ACS Nano* **2011**, *5*, 8943–8949.
- (18) Hu, K.; Xie, X.; Szkopek, T.; Cerruti, M. Understanding Hydrothermally Reduced Graphene Oxide Hydrogels: From Reaction Products to Hydrogel Properties. *Chem. Mater.* **2016**, *28*, 1756–1768.
- (19) Xu, C.; Yuan, R.-s.; Wang, X. Selective Reduction of Graphene Oxide. *New Carbon Mater.* **2014**, *29*, 61–66.
- (20) Mei, X.; Meng, X.; Wu, F. Hydrothermal Method for the Production of Reduced Graphene Oxide. *Phys. E* **2015**, *68*, 81–86.
- (21) Opgenoord, M. M. J.; Caplan, P. C. Aerodynamic Design of the Hyperloop Concept. *AIAA J.* **2018**, *56*, 4261–4270.
- (22) Paredes, J. I.; Villar-Rodil, S.; Martínez-Alonso, A.; Tascón, J. M. D. Graphene Oxide Dispersions in Organic Solvents. *Langmuir* **2008**, *24*, 10560–10564.
- (23) Portier, S.; Rochelle, C. Modelling CO₂ Solubility in Pure Water and NaCl-Type Waters from 0 to 300 °C and from 1 to 300 Bar: Application to the Utsira Formation at Sleipner. *Chem. Geol.* **2005**, *217*, 187–199.
- (24) Cordero, N. A.; Alonso, J. A. The Interaction of Sulfuric Acid with Graphene and Formation of Adsorbed Crystals. *Nanotechnology* **2007**, *18*, 485705.
- (25) Kim, J.; Cote, L. J.; Huang, J. Two Dimensional Soft Material: New Faces of Graphene Oxide. *Acc. Chem. Res.* **2012**, *45*, 1356–1364.
- (26) Kim, J.; Cote, L. J.; Kim, F.; Yuan, W.; Shull, K. R.; Huang, J. Graphene Oxide Sheets at Interfaces. *J. Am. Chem. Soc.* **2010**, *132*, 8180–8186.
- (27) Cote, L. J.; Kim, J.; Tung, V. C.; Luo, J.; Kim, F.; Huang, J. Graphene Oxide as Surfactant Sheets. *Pure Appl. Chem.* **2010**, *83*, 95–110.
- (28) Tung, V. C.; Kim, J.; Huang, J. Graphene Oxide: Single-Walled Carbon Nanotube-Based Interfacial Layer for All-Solution-Processed Multijunction Solar Cells in Both Regular and Inverted Geometries. *Adv. Energy Mater.* **2012**, *2*, 299–303.
- (29) Luo, J.; Tung, V. C.; Koltonow, A. R.; Jang, H. D.; Huang, J. Graphene Oxide Based Conductive Glue as a Binder for Ultracapacitor Electrodes. *J. Mater. Chem.* **2012**, *22*, 12993–12996.
- (30) Martins, V. H. N.; Siqueira, N. M. S.; Fonsaca, J. E. S.; Domingues, S. H.; Souza, V. H. R. Ternary Nanocomposites of Reduced Graphene Oxide, Polyaniline, and Iron Oxide Applied for Energy Storage. *ACS Appl. Nano Mater.* **2021**, *4*, 5553–5563.
- (31) Krishnan, D.; Raidongia, K.; Shao, J.; Huang, J. Graphene Oxide Assisted Hydrothermal Carbonization of Carbon Hydrates. *ACS Nano* **2014**, *8*, 449–457.
- (32) Kim, S. K.; Kim, H.; Chang, H.; Cho, B.-G.; Huang, J.; Yoo, H.; Kim, H.; Jang, H. D. One-Step Formation of Silicon-Graphene Composites from Silicon Sludge Waste and Graphene Oxide Via Aerosol Process for Lithium Ion Batteries. *Sci. Rep.* **2016**, *6*, 33688.
- (33) Jang, H. D.; Kim, S. K.; Chang, H.; Choi, J.-H.; Cho, B.-G.; Jo, E. H.; Choi, J.-W.; Huang, J. Three-Dimensional Crumpled Graphene-Based Platinum-Gold Alloy Nanoparticle Composites as Superior Electrocatalysts for Direct Methanol Fuel Cells. *Carbon* **2015**, *93*, 869–877.
- (34) Ma, H.; Kong, D.; Xu, Y.; Xie, X.; Tao, Y.; Xiao, Z.; Lv, W.; Jang, H. D.; Huang, J.; Yang, Q. H. Disassembly-Reassembly Approach to RuO₂/Graphene Composites for Ultrahigh Volumetric Capacitance Supercapacitor. *Small* **2017**, *13*, 1701026.
- (35) Huang, J. Syntheses and Applications of Conducting Polymer Polyaniline Nanofibers. *Pure Appl. Chem.* **2006**, *78*, 15–27.